1-1-2022

Synthesized copper oxide nanoparticles via the green route act as antagonists to pathogenic root-knot nematode, Meloidogyne incognita

Amir Khan
Aligarh Muslim University

Manar Fawzi Bani Mfarrej
Zayed University

Mohtaram Danish
Aligarh Muslim University

Mohammad Shariq
Aligarh Muslim University

Mohd Farhan Khan
Gagan College of Management and Technology

See next page for additional authors

Green Chemistry Letters and Reviews

ISSN: (Print) (Online) Journal homepage: https://www.tandfonline.com/loi/tgcl20

Synthesized copper oxide nanoparticles *via the* green route act as antagonists to pathogenic root-knot nematode, *Meloidogyne incognita*

Amir Khan, Manar Fawzi Bani Mfarrej, Mohtaram Danish, Mohammad Shariq, Mohd. Farhan Khan, Moh Sajid Ansari, Mohamed Hashem, Saad Alamri & Faheem Ahmad

To cite this article: Amir Khan, Manar Fawzi Bani Mfarrej, Mohtaram Danish, Mohammad Shariq, Mohd. Farhan Khan, Moh Sajid Ansari, Mohamed Hashem, Saad Alamri & Faheem Ahmad (2022) Synthesized copper oxide nanoparticles *via the* green route act as antagonists to pathogenic root-knot nematode, *Meloidogyne incognita*, Green Chemistry Letters and Reviews, 15:3, 491-507, DOI: 10.1080/17518253.2022.2096416

To link to this article: https://doi.org/10.1080/17518253.2022.2096416

Published online: 05 Jul 2022.

GREEN CHEMISTRY LETTERS AND REVIEWS
2022, VOL. 15, NO. 3, 491–507
https://doi.org/10.1080/17518253.2022.2096416

Synthesized copper oxide nanoparticles *via the* green route act as antagonists to pathogenic root-knot nematode, *Meloidogyne incognita*

Amir Khan [a], Manar Fawzi Bani Mfarrej [b], Mohtaram Danish [c], Mohammad Shariq [a], Mohd. Farhan Khan [d], Moh Sajid Ansari [a], Mohamed Hashem [e,f], Saad Alamri [e] and Faheem Ahmad [a]

[a]Department of Botany, Aligarh Muslim University, Aligarh, India; [b]Department of Life and Environmental Sciences, College of Natural and Health Sciences, Zayed University, Abu Dhabi, United Arab Emirates; [c]Department of Chemistry, Aligarh Muslim University, Aligarh, India; [d]Department of Science, Gagan College of Management and Technology, Aligarh, India; [e]Department of Biology, College of Science, King Khalid University, Abha, Saudi Arabia; [f]Botany and Microbiology Department, Faculty of Science, Assiut University, Assiut, Egypt

ABSTRACT

This investigation explains the green synthesis, characterization and biocontrol potential of copper oxide nanoparticles (CuONPs) against second-stage juveniles (J2s) of root-knot nematode, *Meloidogyne incognita* infesting chickpea. Mono-disperse, spherical, pure CuONPs were synthesized from *Jatropha curcas* leaf with particle sizes ranging from 5 to 15 nm in diameter. Antagonistic activities of synthesized CuONPs were studied against *Meloidogyne incognita*. The highest mortality of J2s was found in the 200 ppm concentration of CuONPs at 24 h of exposure. The exact concentration also showed maximum inhibition of J2s hatching from egg masses after six days of exposure. It was worth noting that 25 ppm concentration was the least effective. The pot experiment showed that CuONPs significantly reduced the root infection caused by *M. incognita* and enhanced chickpea plants' growth and physiological attributes (Chlorophyll and carotenoid content). The results depicted when the concentration of CuONPs was increased, J2s mortality rate was also increased. We highlighted the antinematode influence of green synthesized CuONPs. Thus, it will offer an excellent eco-friendly strategy to optimize yield under pathogens attack and provide prospects of green synthesized-based nanoparticles development for pests control. Plants mediated CuONPs will also help in resolving the current toxicity concerns and future challenges in the agriculture.

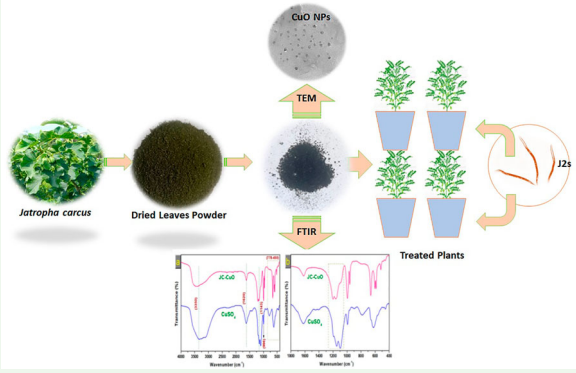

ARTICLE HISTORY
Received 15 December 2021
Accepted 24 June 2022

KEYWORDS
CuO nanoparticle; plant extract; plant-parasitic nematode; nematicidal properties; management

1. Introduction

Pulses seem to be the essential food for vegetarians in the entire world. Pulses are continuously gaining prominence as an affordable protein source and vital for sustainable agriculture. After beans and peas, chickpea (*Cicer arietinum* L.) ranks the world's third among pulse crops, and India accounts for 75% of its global output (*1*). Numerous pathogens significantly reduce chickpea production, including insects, fungi, bacteria, and nematodes (*2*). Root-knot nematodes (RKNs), *Meloidogyne* spp. are the major obstacles to the successful cultivation of chickpea. Among *Meloidogyne* spp., *M. incognita* and *M. javanica* accounting for 19-40% and 24-61% economic losses of chickpea in India (*3*). *M. incognita* has been identified as a substantial yield-reducing pest of economically important crops, having a global

CONTACT Faheem Ahmad ahmad_nematol@yahoo.com, faheem.bt@amu.ac.in Department of Botany, Aligarh Muslim University, Aligarh 202002, India

distribution and a diverse host range that threatened thousands of plant species worldwide (*4*). Treatment of chemical nematicides is usually more effective than other tactics, but their use is restricted because of their toxic effect on the environment and human beings. Therefore, chemical nematicides are losing their attention among farmers as public awareness of their adverse consequences of growth and public views regarding environmental pollution shift. So, there is a need to search for cheap and eco-friendly tactics to sustain agricultural productivity and successfully suppress nematode infestation. Applying nanoparticles synthesized using plant extracts is the best alternative tactic over chemical nematicides (*5*). Due to their specific properties like small size, large surface area, higher chemical reactivity and electric conductivity, nanotechnology-based strategies have recently been deployed to control pathogens (*6*). Copper-based formulations as pesticides have long been used in crop protection. Copper in nano-dimensions renders a considerably greater active form of copper at a substantially lower rate, implying that copper nanoparticles and their composites can potentially control various plant diseases (*7*). Copper and iron are necessary components for the growth of *Capsicum annuum* plants (*8*) because they participate in photosynthesis and other physiological activities at the cellular level, and their absence may result in structural damages (*9*). Presently, plants and their derivatives have attracted great interest in nanoparticle synthesis due to naturally occurring reductants viz., flavonoids, polyphenols, ascorbic acid, and sugars besides carbohydrates and proteins and gums and pectic compounds that act as stabilizing agents (*10*). The field of nanoparticles as nematicidal is a new and emergent area for researchers in agriculture. Nanoagricultureuses nanomaterials in the form of nano pesticides and nano fertilizer in crop protection, providing sustainable options to enhance plant growth (*11*,*12*). Jeyasubramanian (*13*) reported that iron oxide nanoparticles enhanced the growth and productivity of spinach grown in hydroponics. Biosynthesis of metal (Ag, Au, Cu and Cd) nano-formulation of phytoextracts gained significant interest due to their potential use in pest management. Phytoextract-mediated nanoparticles synthesis is always extracellular, and reaction durations are relatively short compared to microbial synthesis. Several plants have been reported for the green synthesis of CuO nanoparticles (*14*–*16*). CuONPs have also been utilized for developing pesticides, herbicides, fertilizers, soil remediation, and growth modulators (*17*). Copper-based nanoparticles demonstrate their efficacy and specificity against various microorganisms (*18*,*19*). Copper nanoparticles and their nanocomposite have also produced a much higher active form of copper and efficiently control plant diseases (*20*). Copper and iron are important minerals in crops and play critical roles in biochemical functions such as photosynthetic electron transport, mitochondrial respiration, oxidative stress, cell wall metabolism, and DNA synthesis (*21*,*22*). The qualitative and quantitative analysis of hexane leaves extract of *J. curcas* through GC-MS revealed the presence of different alcohols, hydrocarbons, esters, ketones and other compounds (*23*,*24*). These major extracted components identified in the analysis act as capping and stabilizing agents for the biosynthesis of JC-Cu NPs. They may also be responsible for reducing Cu^{+} to Cu^{0} and cause a broad absorption spectrum (*25*). Moreover, the quantity and content of active components in biological extracts determine the dimensional appearance of nanoparticles (*26*,*27*). Information from recent developments about the CuONPs synthesis *via* green route, characterization and applications from previous scientific findings against various pathogenic microbes acclaimed advantages and considered eco-friendly non-toxic materials. Thus, there is a need to implement new agricultural practices that provide sustainable resources and maintain healthy soil microbiota. Current researchers are working to produce the food systems sustainably by using green strategies in agriculture to control pests and diseases. The green strategy is a more environmentally-friendly formulation, and this approaches also have the potential to provide effective solutions to multiple problems of agriculture crops. In this context, an attempt was made to synthesize copper oxide nanoparticles (CuONPs) by greener route using the *Jatropha curcas* leaves extract instead of harmful reducing or capping agents. We also characterized green synthesized CuONPs and investigated their antagonistic potential towards RKN, *M. incognita*.

2. Materials and methods

2.1. Materials

The RKN, *Meloidogyne incognita,* was selected as a target pathogen, and chickpea (*Cicer arietinum* L.) was used as a test plant. Fresh leaves of *J. curcas* were used for the green synthesis of CuONPs. The chemicals used in the synthesis procedure, such as copper (II) sulphate (CuSO4), were bought from Sigma Aldrich.

2.2. CuONPs biosynthesis

Fresh leaves of *J. curcas* were collected from our University Campus, washed with double distilled water (DDW) to eliminate the impurities on the surface and dried in

the dark for approximately ten days. An electric mixer was used to grind the leaves into fine powder. Ten grams (10 g) of obtained fine powder were mixed with 150 mL of DDW and heated in a flask for 90 min at 70° C. After this, the colored solution was cooled to ambient temperature and filtered. 100 mL of the freshly obtained colored extract was mixed with 100 mL of one molar (1M) copper sulphate solution and stirred at 90°C for 120 min. Within the stipulated period, the color changed as a function of time, indicating the synthesis of CuONPs via reduction route through the copper salts viz. $CuSO_4$ reduction (Figure 1). The mixture was centrifuged at 5000 rpm after the desiring reaction time for 20 min, and obtained nanoparticles dried at 150°C for 12 h. Figure 1 depicts the main steps of the biological extract collection and the synthesis of CuONPs. The nucleation process allowed the formation and release of CuONPs at a temperature above 100°C, dissolved 10 mg of CuONPs in 10 mL of Dimethyl sulfoxide (DMSO). This solution named as stock solution, prepared different concentrations (25, 50, 100 and 200 ppm) of CuONPs by adding the required DDW for further study.

2.3. CuONPs characterization

Fourier transforms infrared (FTIR) spectrophotometer (Perkin Elmer Spectrum 2) was used to obtain information about bonding in the molecular structure of prepared samples using KBr powder as reference material. An X-ray diffractometer (Shimadzu XRD, model 6100) with Cu radiation [Cu Kα radiation, (1.540 Å)] of 15 mÅ current and scanning rate 10^{o}/min was used for valuation of the phase structure of prepared material.

The qualitative optical properties of the *J. curcas* extract and bio-synthesized CuONPs are examined by a non-destructive technique viz. UV–vis Diffuse Reflectance spectroscopy (DRS) using the Perkin-Elmer-Lambda 35 UV–vis DRS spectrophotometer. The electronic transitions of the sample molecules enable the spectra of *J. curcas* extract to be recorded efficiently. UV-Vis spectrometers often measure the transmittance or absorbance of a transparent substance or solution. The sample size for this mode of measurement absorbance/transmittance is about 1–2 mg (solid part)/ 1–2 ml (liquid other than water). The method entailed projecting light with known spectral energy onto an extract sample held at a right angle to the light source and measuring the intensity of the reflected light with photo detectors (*28*–*30*). The Perkin-Elmer-Lambda 35's variable band width provided good results for experiments on *J. curcas* extract and bio-synthesized CuONPs.

A JEOL JSM-6510LV-SEM with a 50 kV voltage (from JEOL Co. Ltd. Japan) was utilized to examine the surface morphology of the sample. The particle structure of the samples was analysed using a JEOL-JEM-2100 transmission electron microscope (TEM) at 200 Kv (also from JEOL Co. Ltd. Japan). The specimens for the TEM investigations are made by depositing a drop of pulp colloidal solution on an approx. 400 mesh grid coated with an amorphous C-sheet and evaporated the liquid part at room temperature followed to determine the exact form and size of the CuONPs.

2.4. Multiplication and collection of J2s

The pure culture of RKN, *M. incognita,* was well-maintained on brinjal in the glasshouse. The nematode infected brinjal roots were used to pick egg masses using sterilized forceps. The obtained egg masses were washed with DDW and poured into 25 µm pore size mesh sieves with a cross-layer of tissue paper put in Petri plates containing DDW. These Petri-plates were kept in a BOD incubator to hatch second-stage infective juveniles (J2s) of *M. incognita*. The mesh retained the egg masses while the hatched J2s moved through the sieve and sank to the Petri plate's bottom. According to our previously described procedure (*31*), fresh hatched J2s were obtained from Petri plates and stored for further study. J2s were used for further experiments within five days from the storage date.

2.5. SEM analysis for Meloidogyne species identification

Scanning Electron Microscopy was used for the identification of *M.incognita* species. A mature female of *M. incognita* separated from the infected root of eggplant, and the perineal pattern was prepared using the method given by Abrantes and Santos (*32*). The perineal pattern was coated with 14 nm of gold, and SEM images were taken using SEM (JSM 6510 LV Jeol-Japan) analysis. The morphology of the perineal pattern of *M. incognita* was studied to characterize the *Meloidogyne* species (Figure 2). The key features of the perineal pattern include an angularly oval structure with a high dorsal arch in a typical pyriform. Striae were in distinct waves which bent towards lateral lines and were not interrupted. Striae were straighter with an oval appearance in ventral regions.

2.6. Mortality bioassay

In the mortality test, the hatched J2s were treated with different concentrations of CuONPs viz., 25, 50, 100, and 200 ppm. Each treatment had five replicates. To determine mortality, 1 ml of DDW containing 90

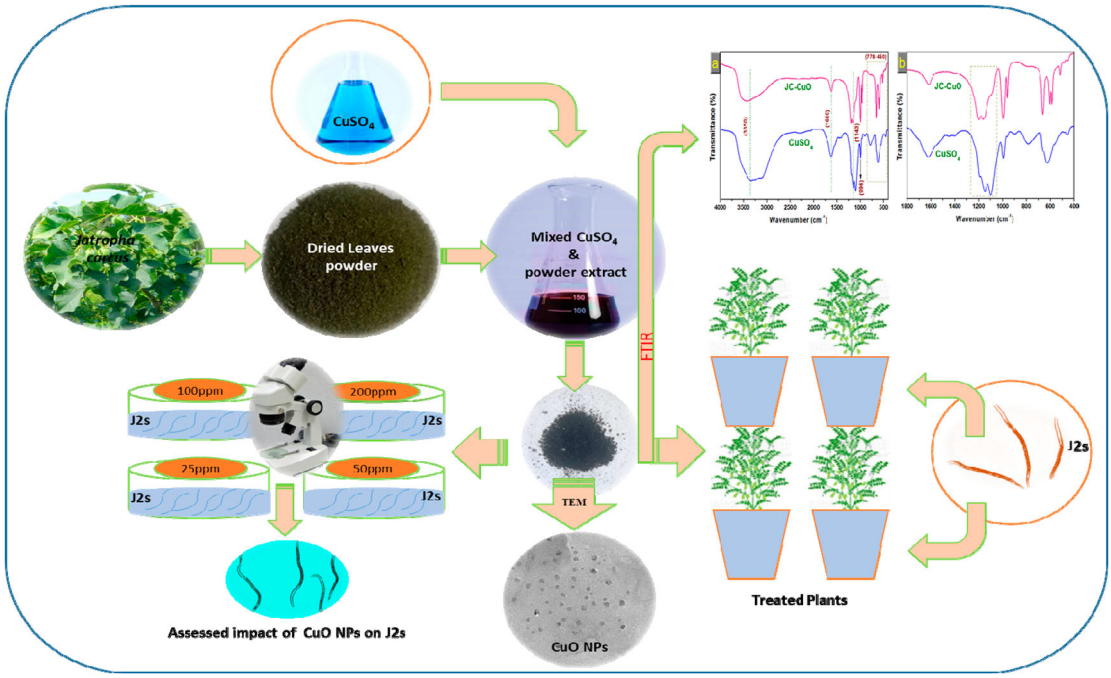

Figure 1. Flowchart represents the various stages employed in the bio-synthesis of CuONPs using *J. curcas* leaves to assess antinematode properties.

freshly hatched J2s was poured into Petri dishes containing 9 ml of the different concentrations of CuONPs separately. These Petri plates were incubated at 28°C for 8, 16, and 24 h of exposure. After the exposure time, the counting was started using a stereoscopic microscope to determine the living and dead J2s. Those J2s showed any mobility or looked as winding shape were considered alive, and if J2s did not display any motion

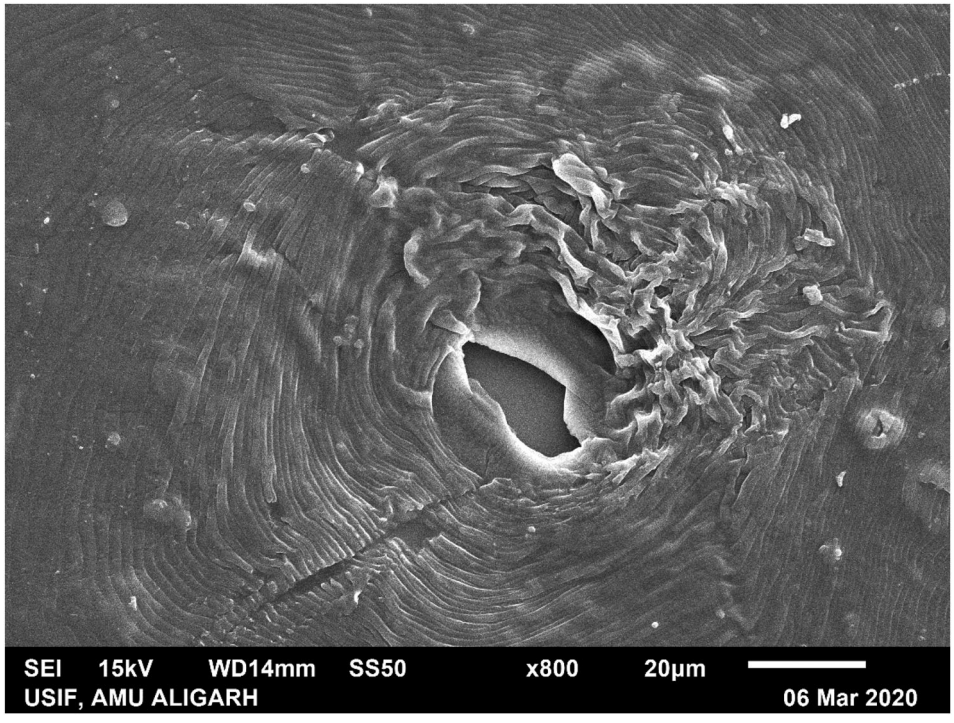

Figure 2. Scanning electron microscopy showing the perineal pattern of *M. incognita*. The high squared dorsal arch, wavy striae are key features of *M. incognita*.

and their body shape viewed straight, then found them as dead (33) and calculate the per cent mortality using the following formula:

$$\text{Percent Mortality} = \frac{C_0 - T\alpha}{C_0} \times 100$$

where, C_0 = Number of live J2s in control; $T\alpha$ = Number of live J2s after 8, 16, and 24 h of exposurein different CuONPs concentrations

2.7. Hatching bioassay

For the hatching test, six healthy egg masses of *M. incognita* were handpicked from the infected root of brinjal and transferred into Petri dishes containing 10 mL of different concentrations of bio-synthesized CuONPs. Petri dishes were incubated for six days at 28°C to allow egg hatching. In the control set-up, six egg masses pour in DDW. Each treatment had five replicates. After six days of exposure, the hatched J2s were counted in each treatment with the help of a stereomicroscope (Zeiss, Carl Zeiss Microscopy GmbH, Germany) and calculated the per cent inhibition in egg hatching using the formula (34).

$$\text{Percent inhibition} = \frac{C - T}{C} \times 100$$

where, C = Number of hatched J2s in control set-up; T = Number of hatched J2s in different concentrations of CuONPs

2.8. Infectivity bioassay and experimental design (Pot study)

The pots designed study was conducted in a glasshouse to determine the nematode-toxic efficacy of bio-synthesized CuONPs against *M. incognita*. Seeds of chickpea cv. 'Avarodhi' was purchased from the market. Chickpea seeds were sterilized using 0.02% mercuric chloride by shaking for 5 min and instantly washed with running tap water 2–3 times. Clay Pots (15 cm in diameter) filled with 1 kg autoclaved mixed soil of loam and farmyard manure in proportion 3:1. Five sterilized seeds of chickpea cv. 'Avarodhi'were sown in pots. After germination, we gently pulled out the unwanted seedlings, leaving the one healthiest in each pot. We placed the 2–3 holes around the seedling's root and inoculated with 2500 J2s. After two days of J2s inoculation, 10 ml of different concentrations (25, 50, 100, and 200 ppm) of CuONPs were added around the seedling's root using a pipette. Plants were watered satisfactorily and irrigated sufficiently throughout the experiment and carefully followed the study to eliminate errors during the examination. The treatments include (a) Control (No CuONPs and J2s); (b) Untreated inoculated control (Nematode only); (c) Ten milliliter of 25 ppm of CuONPs + 2500 freshly hatched J2s; (d) Ten milliliter of 50 ppm of CuONPs+ 2500 freshly hatched J2s; (e) Ten milliliter of 100 ppm of CuONPs+ 2500 freshly hatched J2s; (f) Ten milliliter of 200 ppm of CuONPs + 2500 freshly hatched J2s.

2.9. Estimation of growth, yield, and physiological attributes

At maturity, plants were harvested and washed with running tap water to eliminate sticky soil particles, and assessments were made to analyse the growth, yield and physiological attributes. In terms of growth parameters (plant length, fresh plant weight, pods number), photosynthetic pigments chlorophyl and carotenoid content (mg/g) determined following the methods described by Mackinney (35) and MacLachlan and Zalik (36), respectively.

2.10. Determination of pathological parameters (Root galls and nematode population)

The root galls were visually counted. At harvesting time, the estimation of the final population of J2s in 200 g of soil was determined by Cobb's sieving and decanting technique (37), followed by modified Baermann's funnel technique (38).

2.11. Statistical analysis

A completely randomized design was used for the pots study. All data are expressed as mean ± Standard error mean (SEM). Statistical analysis was conducted using R software (version 2.14.1), one-way analysis of variance (ANOVA) with Duncan Multiple Range Test (DMRT) to find significant differences ($P < 0.05$). The Principal Component Analysis (PCA) was done using Origin software [version 2019b (9.65)].

3. Results and discussion

3.1. Biosynthesis of CuONPs via the green route

Leaves extract of *J. curcas* contains biomolecules such as tannins, saponins, coumarin, phenols, and alkaloids that play a significant role in capping and stabilizing agents during the bio-synthesis of CuONPs. Several biomolecules including p-Dioxane-2,3-diol, Benzene, 2-benzyloxy-1-methoxy-4 (2nitroethenyl), Octadecenoic acid, Methyl stearate, Benzenamine, Acetophenone, Octadecenoic acid, alpha-Benzamido-2-hydroxycinnamic acid,

(2E,4E)-N-Isobutyltetradeca-2,4-dienamide, Hexadecanoic acid methyl ester, were identified from the plant extract of *J. curcus* through GC-MS analysis (*39*,*40*). These phytochemicals have been used as the antagonist for pathogenic microbes, including plant pathogens (*41*,*42*). Aside from the antagonistic properties, one of the past reports revealed that these biomolecules also influence the size of nanoparticles (*43*) and can also form strong bonds with metallic ions. Therefore, these are promising agents which could play a significant role in nanomaterial synthesis *via* the green route. The flowchart for the bio-biosynthesis of CuONPs is given in Figure 1. The Color change indicates the synthesis of CuONPs *via* the reduction route through copper salts, namely $CuSO_4$ reduction. The UV peaks successfully demonstrated that *J. curcas* macromolecules act as capping and stabilizing agents in the biosynthesis of CuONPs by reducing Cu^{2+} ions to Cu^0.

$$Cu^{2+}\text{ions} \xrightarrow[\text{Stabilizers / Capping Agents}]{\text{Tannins/ Saponins/ Coumarin/ Phenols/}} Cu^0 \qquad \text{(a)}$$

Cu^0 formed could be oxidized to Cu_2O and CuO (*44*). When the Cu^0 react with the dissolved oxygen molecules in the aqueous solution, this oxidation reaction occurs quickly as:

$$Cu^0 + O_2 \rightarrow Cu_2O \qquad \text{(b)}$$

$$Cu^0 + O_2 \rightarrow CuO \qquad \text{(c)}$$

Cu_2O, on the other hand, is slightly more stable than CuO in the solid-state, as evidenced by their standard formation enthalpies, i.e. $\Delta_f H^{\theta}(CuO) > \Delta_f H^{\theta}(Cu_2O)$. That's why excess Cu^0 may cause copper (II) oxide to be reduced to copper (I) oxide nanoparticle (*45*)

$$CuO + Cu \rightarrow Cu_2O \qquad \text{(d)}$$

Furthermore, oxidation of copper (I) oxide is possible if the working pH is significantly larger than alkaline and the average temperature remains unchanged (*46*)

$$Cu_2O + O_2 \rightarrow CuO \qquad \text{(e)}$$

To repeat, *J. curcas* leaves extract contains biomolecules such as tannins, saponins, coumarin, phenols, and alkaloids, which are important capping and stabilizing agents during the biosynthesis of CuONPs.

3.2. Characterization of bio-synthesized CuONPs

3.2.1. Fourier transform infrared spectroscopy (FTIR) analysis

The role of *J. curcas* phytochemicals functional groups in the capping and synthesis of CuONPs via reduction route was investigated using FTIR spectroscopy. This analysis was carried out within 400-4000 cm^{-1}better to understand chemical structure and bonding interaction in bio-synthesized CuONPs. Peaks were found at 3500, 1620, 1145, 1143, 996 and narrow band between 778 and 450 cm^{-1}, as shown in Figure 3(a). The absorbance band at 3500 $cm^{-1}$is associated with phenolic substances' O-H intermolecular stretching bond. The peak at 1620 cm^{-1} is attributed to the C = C bond of the conjugated alkene. FTIR absorbance spectra for bio-synthesized CuONPs was also exhibited band at 1145 and 1143 $cm^{-1,}$ respectively, for characteristics of the C–O stretch. The band of some functional groups shifted to a higher value, suggesting that leaves extract interacted with the copper sulphate ions. The peak intensities of the phytochemical-capped bio-synthesized CuONPs decreased; hence, those groups' apparent involvement in the bioreduction route and stabilization of CuONPs. The presence of phytochemicals in *J. curcas* leaves extract binds with the metals through various functional groups and forms a coating layer around the metal nanoparticles, preventing agglomeration and stabilizing the metal nanoparticles (*47*,*48*). Several studies reported similar findings (*49*–*51*).

3.2.2. X-ray diffraction (XRD) analysis

XRD confirmed the phase structure, crystalline nature, and purity of CuONPs. XRD pattern of green synthesized CuONPs was recorded using XRD instrument and operated at 30 kV voltage and 15 mA current with graphite monochromatic radiation [Cu Kα radiation (1.540 Å)], at 10°/min output speed in range 20-70° at the value of 2θ. The XRD data are displayed in Figure 4(a). The peaks corresponding to 2θ values of 26.98, 30.73, 31.75, 31.85, 46.87, 56.49, and 65.94° which could be ascribed to the (021), (110), (002), (111), (−202), (020) and (−311) lattice planes, respectively, suggesting that material is polycrystalline and well consistent with JCPDS card no. 89-5895, indicating a monoclinic structure of CuONPs (*52*–*54*). No other phases corresponding to impurities were observed, suggesting that high purity of CuONPs were successfully synthesized. The XRD pattern of pure copper sulphate is shown in the inset graph (Figure 4b), which better agrees with previous results (*55*). The average particle size of CuONPs has also been calculated with the help of XRD data using the Scherrer formula (Eq. 1) (*56*,*57*). $D = K\lambda/\beta\ Cos\theta$; Where λ = wavelength of X-ray radiation (0.15418); β = FWHM (full-width half-maxima); D and K = crystallites size and Scherrer constant (0.94), respectively. Sharp XRD patterns showed that CuONPs have a crystallite size of 84 ± 2 nm.

3.2.3. UV-Vis DRS analysis

The UV-vis DRS spectroscopy has been used to examine optical properties of bio-synthesized CuONPs

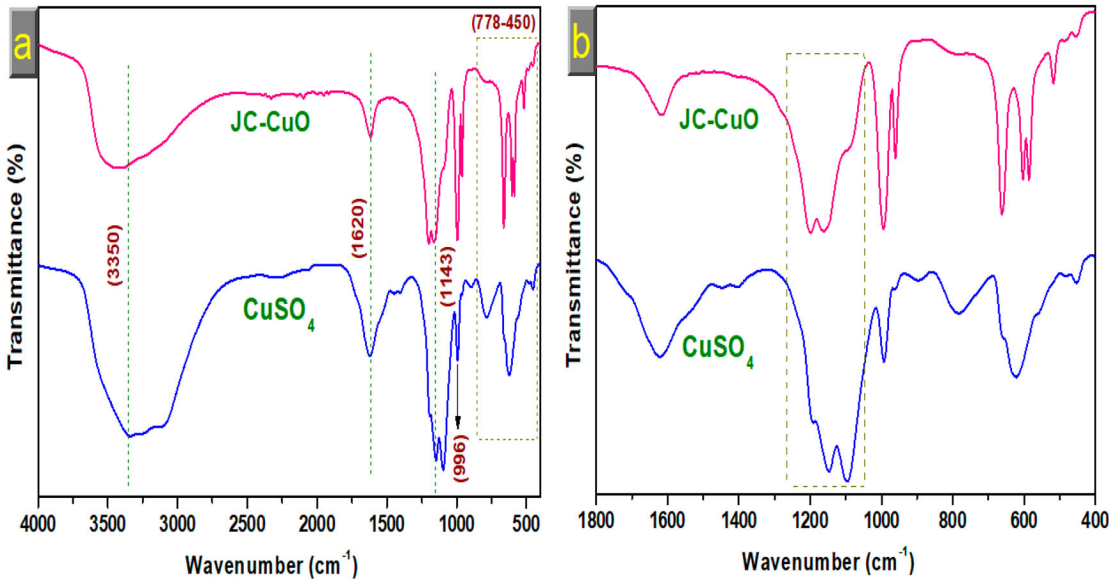

Figure 3. (a) FTIR spectra of pure copper sulphate and CuONPs (b) corresponding magnified FTIR spectra.

by using Perkin-Elmer-Lambda 35 UV–vis spectrophotometer. The DRS spectra of *J. curcas* leaves extract and bio-synthesized CuONPs have been examined in the 200–700 nm range, and outcomes are displayed in Figure 5. The DRS spectra of *J. curcas* leaves extract was observed in the region of 250-300 nm, whereas bio-synthesized CuONPs appeared in a region of 300–400 nm, reveals that a bathochromic shift (or the red-shift) compared to *J. curcas* leaves extract, which might be due to extracts interacted with copper sulphate ions. The distortion peaks were also observed, which might be caused by proteins involved in nanoparticle reduction routes and capping (*58*,*59*). The UV peaks successfully revealed that *J. curcas* macromolecules serve as capping and stabilizing agents in the bio-synthesis of CuONPs by reducing Cu^{2+} ions to Cu^{0}.

3.2.4. Scanning electron microscopy (SEM) analyses

SEM study was conducted to analyse the morphology and structure of CuO nanoparticles (CuONPs). The results are shown in Figure 6 (a-d). The SEM micrograph of various magnifications viz. (a) 10 µm, (b) 5 µm, (c) 1 µm and (d) 0.5 µm, revealed the rough but continuous geometries of plant extracts surfaces of *J.curcas* leaves holding CuONPs. It is noticeable that *J. curcas* extracts leaf extracts appear to reduce agglomeration of the nanoparticles to a lesser extent (*59*). The TEM results demonstrated that CuONPs supplied higher homogeneity across the entire sample. Obtained results were analysed according to the magnified microphotographs from the several randomly chosen locations.

3.2.5. Transmission electron microscopy (TEM) analyses

The TEM micrograph (Figure 7) further shows that the CuONPs biosynthesis resulted in a consistent distribution of nanoparticles throughout the surfaces of *J. curcas* extracts. Inset in Figure 7 represented the CuONBs more intricately owing to their crystalline nature. The micrograph depicts regular geometries of *J. curcas* extracts carrying a considerable amount of CuONPs in the semi-hardened pulp. However, the exact form and size of CuONPs are determined using TEM. The average diameter of the prepared CuONPs was found between 5 and 15 nm in enlarged microphotographs in different arbitrarily chosen sites. CuONPs nanosized and a considerable distance between the CuONPs prompted them to show their efficacy against J2s infection in chickpea plants. The bio-synthesized CuONPs have enough surface area and more space to reduce J2s activities around the roots.

3.2.6. High resolution-transmission electron microscopy (HR-TEM) analyses

The morphology and microstructure of biosynthesised CuONPs were further examined by high-resolution transmission electron microscopy (HR-TEM, JEOL JEM-2100F). The two HR-TEM images at low and high magnifications [(a)20 and (b)5 nm]were analysed (Figure 8). The HR-TEM images demonstrate the formation of bio-synthesized CuONPs, and the morphologies are consistent with TEM analyses. Moreover, we were also observed that synthesized nanoparticles have a regular shape and homogeneous size distribution in a large domain.

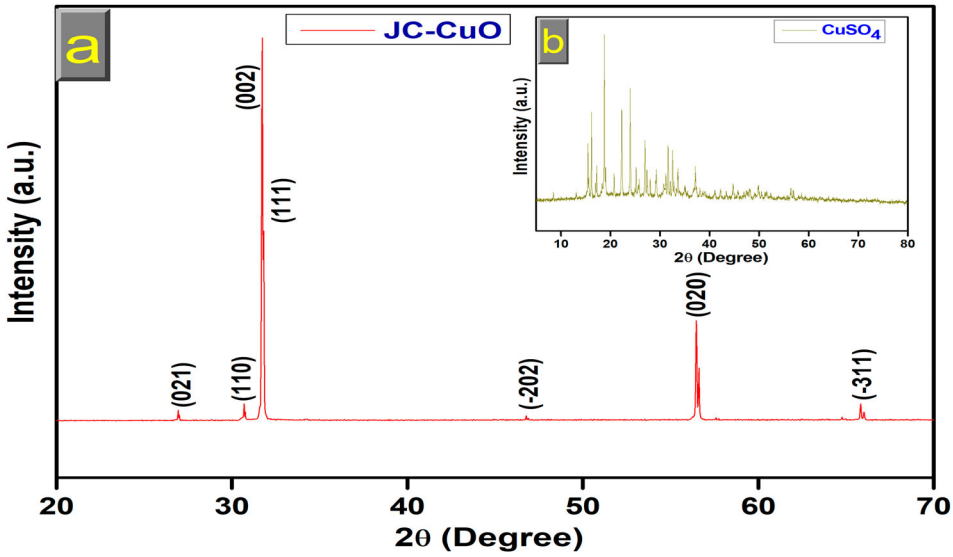

Figure 4. (a) XRD spectra of CuONPs (b) inset of copper sulphate XRD spectra

3.3. Assessment of the nematicidal effect of different concentrations of biosynthesised CuONPs

The influence of different concentrations of bio-synthesized CuONPs was assessed against J2s mortality. The findings showed a noticeable impact of the different concentrations of 25, 50, 100, and 200 ppm on mortality of J2s at different exposure times viz., 8, 16, and 24 h. The significant results were obtained at $P < 0.05$ and are shown in Table 1. We compared the results with control because no mortality of J2s of *M. incognita* has been reported in the control set-up. However, the result revealed that J2s mortality was increased as we extended the exposure period, and sixty per cent of J2s mortality was reported at 24 h of exposure when treated with 200 ppm CuONPs. We noticed that J2s mortality was proportionally related to the CuONPs concentrations and exposure period. However, lower concentrations of CuONPs *viz.*, 25 and 50 ppm were, also showed significant J2s mortality compared to control (Table 1).

J2s hatching inhibition bioassay was also conducted at different concentrations of bio-synthesized CuONPs

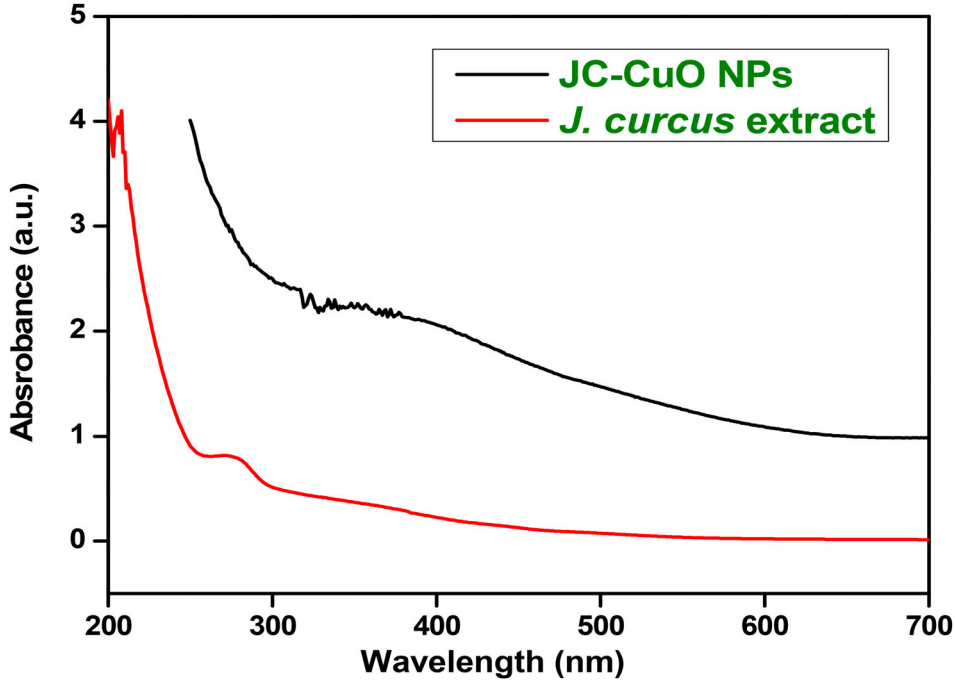

Figure 5. UV-Vis DRS spectra of the *J. curcas* leaves extract and synthesized CuONPs.

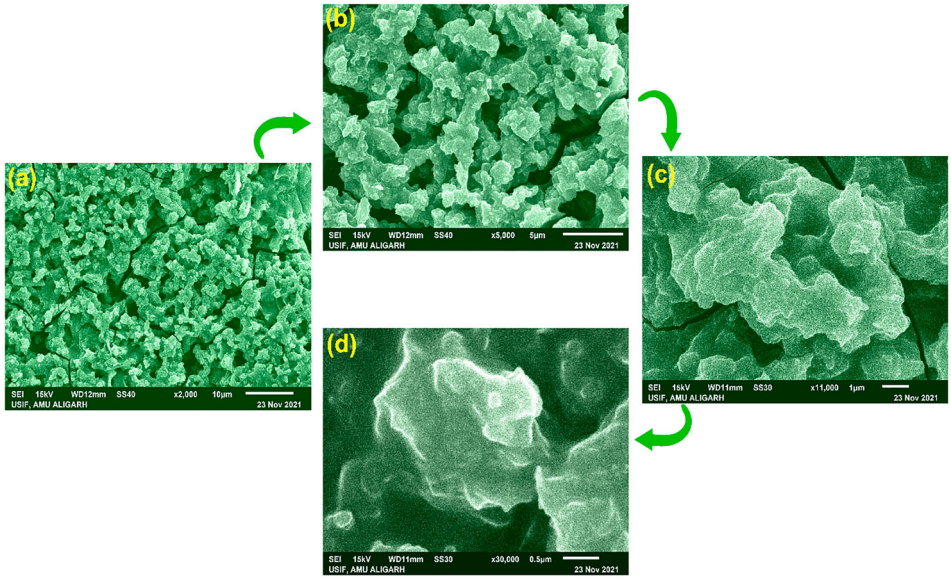

Figure 6. SEM images of green synthesized CuONPs using *J. curcas* leaves. Images displayed at different magnifications level (a) 10 µm, (b) 5 µm, (c) 1 µm and (d) 0.5 µm.

viz., 25, 50, 100, and 200 ppm. We were analysed using a direct contact method for six days and noticed a significant difference in J2s hatching inhibition among tested treatments (Table 2). In this bioassay, 200 ppm treatment showed the highest per cent inhibition of J2s hatching from egg masses of *M. incognita*. However, other concentrations viz., 25, 50 and 100 ppm also exhibited significant hatching inhibition than control. Inhibition in the J2s hatching from egg masses increased when concentrations increased from 25 to 200 ppm. The individual inhibitory effect of all applied treatments of CuONPs in J2s hatching is presented in Table 2.

We found that CuONPs caused J2s mortality and induced inhibition in J2s hatching, and based on the obtained impact of CuONPs against J2s, predicts the nematicidal potential of green synthesized CuONPs. Mohamed et al. (*60*) reported that different concentrations of copper nanoparticles caused J2s mortality of *M. incognita*. Akhter et al. (*61*) findings regarding the impact of Cu NPs against J2s and egg hatching of *M. incognita* resemble our reports of this study. A similar finding by Eloh et al. (*62*) have also been reported on the nematicidal potential of copper salts with maleimide derivatives against *M. incognita*. The nematodetoxic action of CuONPs on *M. incognita* can be due to multiple mechanisms like disrupting several cellular mechanisms and permeability of the membrane, synthesis of ATP, and oxidative stress response (*63–65*). Validation supposed regarding J2s mortality can disrupt the cellular organization of nematodes induced by applied nanoparticles. Ma et al. (*66*) observed that heavy metals negatively impacted *Caenorhabditis elegans* by breaking down cell membrane integrity and shifting the cations associated with proteins. Copper ion and other metals affect the neuron's function due to condensed cellular energy by fluctuating mitochondrial activity, improving stress by ROS production, and activating cell death paths like apoptosis, and necrosis (*67*). The outcome of our study suggests that bio-synthesized CuONPs could be directly or indirectly used against root-knot nematodes that cause crop yield loss.

3.4. Stability of bio-synthesized CuONPs on *M. incognita*

The stability of bio-synthesized CuONPs is a significant parameter for practical application. Therefore, we have assessed the nematicidal potential of the bio-synthesized CuONPs for multiple cycles. As presented in Figures 9(a and b), the nematicidal potential of bio-synthesized CuONPs showed excellent stability up to the fourth consecutive cycle, and no significant loss occurred. It was observed that a minute decrease in the number of dead J2s at 200 ppm (Figure 9a) and a slight increase in the number of J2s hatched at 200 ppm (Figure 9b) was seen, which might be due to the loss of NPs amount in the course of recovery and partial deactivation after several runs. Ninety living J2s and six egg masses were used at 200 ppm concentration under each experimental run. NPs were separated by centrifugation, followed by water and ethanol washing. The above results made it clear that bio-synthesized CuONPs could be considered a stable catalyst for potential nematicidal ability.

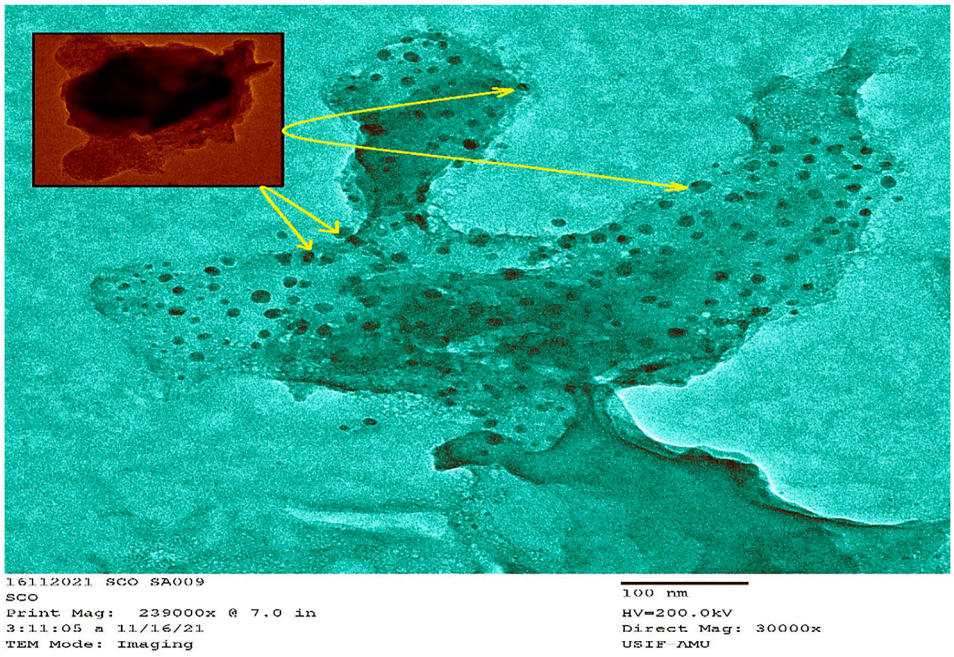

Figure 7. TEM images of green synthesized CuONPs using *J. curcas* leaves.

3.5. Role of green synthesized CuONPs on improving growth, yield and physiological attributes of chickpea and in reduction of pathological parameters

All tested concentrations of bio-synthesized CuONPs viz., 25, 50, 100, and 200 ppm significantly improved the growth attributes of chickpea like plant length, plant fresh weight, and the number of pods/plant. Treatment of 200 ppm CuONPs showed maximum enhancement in the above growth attributes among all applied treatments. Other used treatments 25, 50 and 100 ppm also showed improvement in all growth attributes compared to that pot inoculated with only J2s. The chickpea plants displayed a diverse response to applying different concentrations of CuONPs (Figure 10). Similarly, significant chlorophyll and

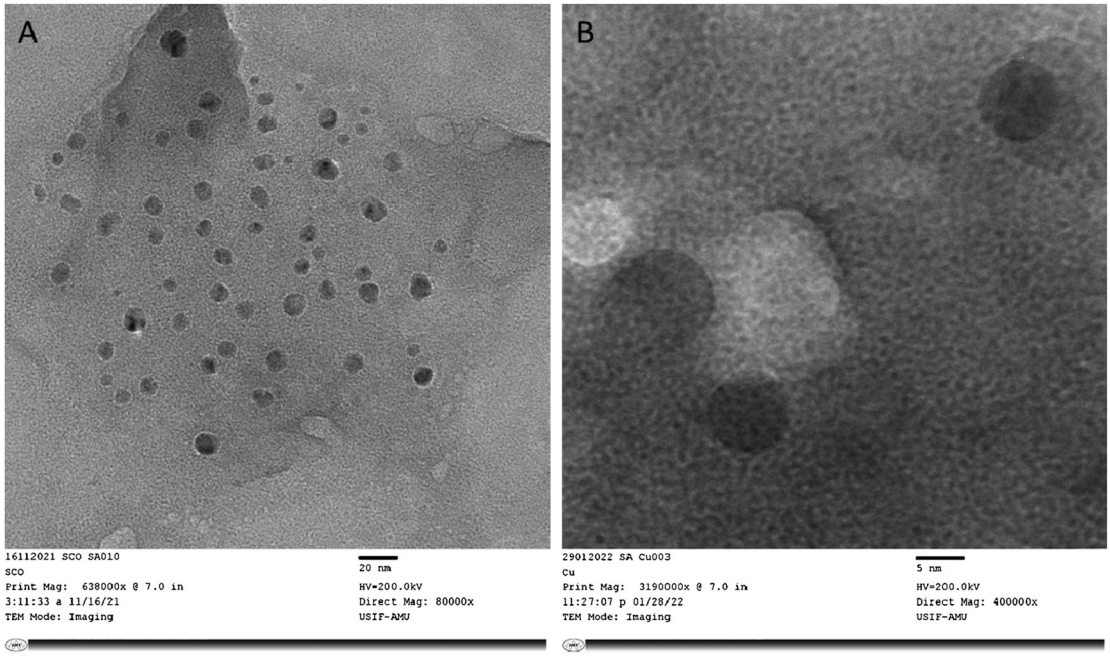

Figure 8. HR-TEM images of green synthesized CuONPs using *J. curcas* leaves. The image captured at (a) low (20 nm) and (b) high magnification (5 nm).

Table 1. Antagonistic effect of different concentrations of bio-synthesized CuONPs towards J2s mortality of M. incognita. The J2s mortality was measured at 8, 16 and 24 h exposure periods.

		Number of J2s dead in different concentrations (ppm)				
Treatment	Incubation (Hours)	200 ppm	100 ppm	50 ppm	25 ppm	DDW (Control)
CuONPs	08	36a±2.64 (40.0%)	24b±2.30 (26.7%)	17c±2.64 (18.9%)	11d±1.73 (12.2%)	0 ± 0 (0%)
A.	16	51a±2.88 (56.7%)	39b±2.08 (43.3%)	30c±2.30 (33.3%)	21d±2.08 (23.3%)	0 ± 0 (%)
	24	76a±2.64 (84.4%)	56b±3.00 (62.2%)	43c±1.73 (47.8%)	34d±2.64 (37.8%)	0 ± 0 (%)

Each value is an average of five replicates; SE-Standard error; DW-Distilled water (control); ppm-Parts per million; Values are given in parentheses represent per cent J2s mortality over control.; Values are given without parentheses representing the number of the dead J2s.

Table 2. Inhibitory effect of different concentrations of CuONPs on J2s hatching from egg masses of M. incognita after six days of incubation.

	Number of J2s(mean ± SE) hatched in different concentrations (ppm)				
Treatment	200 ppm	100 ppm	50 ppm	25 ppm	DDW (Control)
CuONPs	76e±4.93 (80.0%)	98d±6.08 (74.2%)	122c±5.29 (67.9%)	148b±8.08 (61.1%)	380a±7.57 (0.0%)

Each value is an average of five replicates; SE-Standard error; DW-Distilled water (control); ppm-Parts per million; Values are given in parentheses represent per cent inhibition in J2s hatching over control; Values are given without parentheses representing the hatched J2s.

carotenoid content enhancement were observed at 200 ppm treatment (Figure 11). Other treatments like 25, 50 and 100 ppm also showed an increase in chlorophyl and carotenoid content compared to that pot inoculated with only J2s. Plants inoculated with J2s only exhibited the highest chlorophyl and carotenoid content reduction.

In the case of pathological parameters (root galls and J2s population), bio-synthesized CuONPs were applied, significantly scaling down root galls and J2s population in soil compared to that pot inoculated with only J2s (Figure 12). The maximum reduction of root galls was found at 200 ppm followed by 100 ppm, 5 0 ppm, whereas the least was at 25 ppm. Similarly, 200 ppm treatment was most prominent in decreasing J2s population followed by 100, 50 and 25 ppm. Those pots inoculated with 2500 J2s only showed the highest root galls and J2s population. The outcome of the principal component analysis showed that the RKNs population in soil and root galls per plant was strongly correlated with other parameters of chickpea. Scatter biplot showed that different concentrations of CuONPs were found highly effective, reduced the root infestation caused by *M. incognita* considerably, and improved chickpea's growth attributes (Figure 13).

The outcome of the present study established the antagonistic activity of bio-synthesized CuONPs. Thus, it could be used to manage root-knot infection. Earlier reports proved that the developed biological materials are responsible for the non-presence of root exudates, causing minor attraction of J2s towards roots (*68*). Furthermore, copper is essential for plant growth, regulating photosynthetic responses, enzyme and transcription activation. It was reported that copper applied in a lesser amount boosts plant growth and act as a micronutrient (*69*). The application of copper improved morphological traits in maise (*70*).

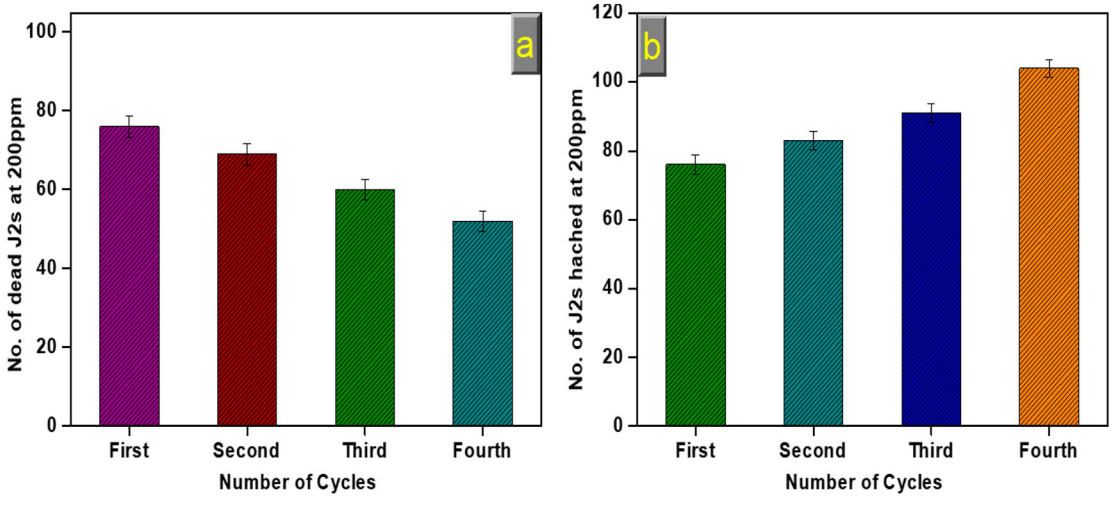

Figure 9. Figure showing the recyclability results of bio-synthesized CuONPs against J2s of *M. incognita* (a) Dead J2s at 200 ppm,(b) hatched J2s at 200 ppm.

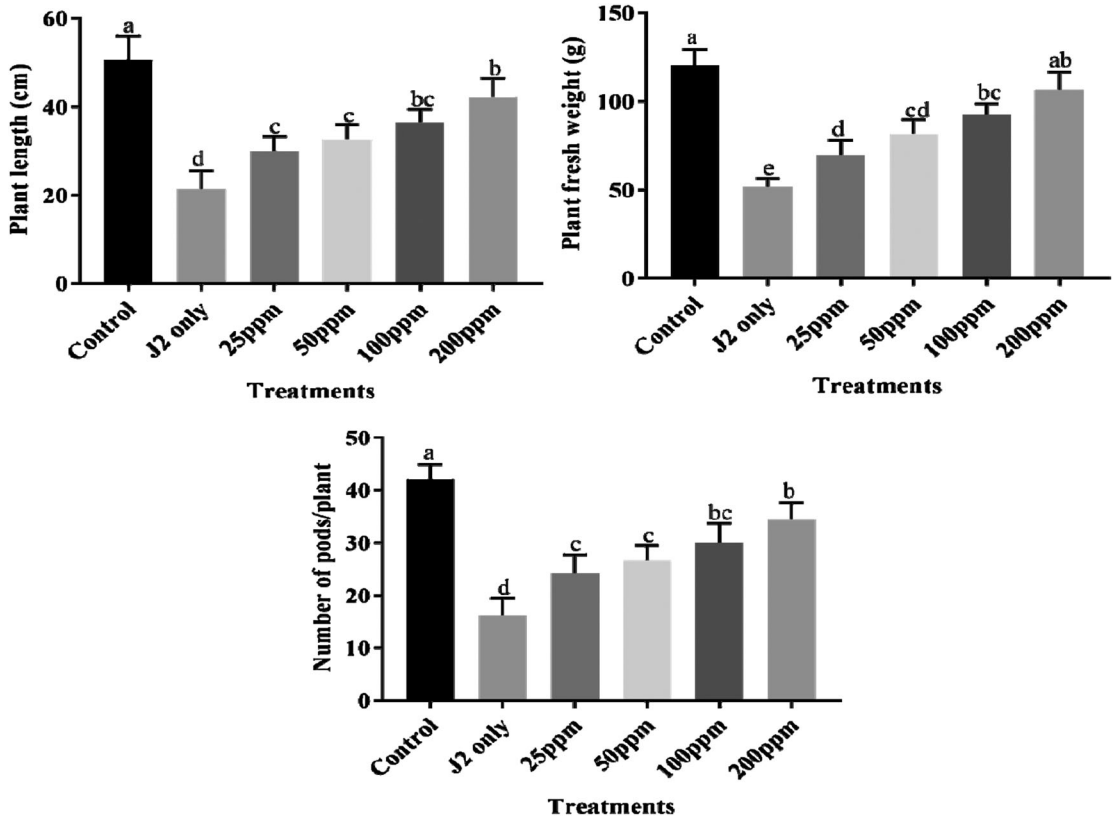

Figure 10. Nematicidal effect of different concentrations of green synthesized CuO NPs on the growth attributes of J2s inoculated chickpea plants.

Copper applied at 0.1% concentration with other nutrients showed a significant increase in shoot attributes of wheat (*71*). In their study, Yeon et al. (*72*) found that combined maleic acid and copper sulphate combined application suppressed RKNs disease on tomatoes by 51.72% and subsequently decreased gall development on melon and population of nematode in soil. Gkanatsiou et al. (*73*) reported that copper/iron-based nanoparticles act as bioactive agents against *Meloidogyne* spp. as well showed plant improvement assets on nematode-infested tomato. Tauseef et al. (*74*) reported in their study that treatment with CuO nanoparticles improves the growth and physiological parameters of cowpea and reduced galls, egg masses and J2s population of *M. incognita*. Synthesized copper oxide nanoparticles of *Elodea densa* improved photosynthesis ratio when applied at minor applications, while a higher amount showed a

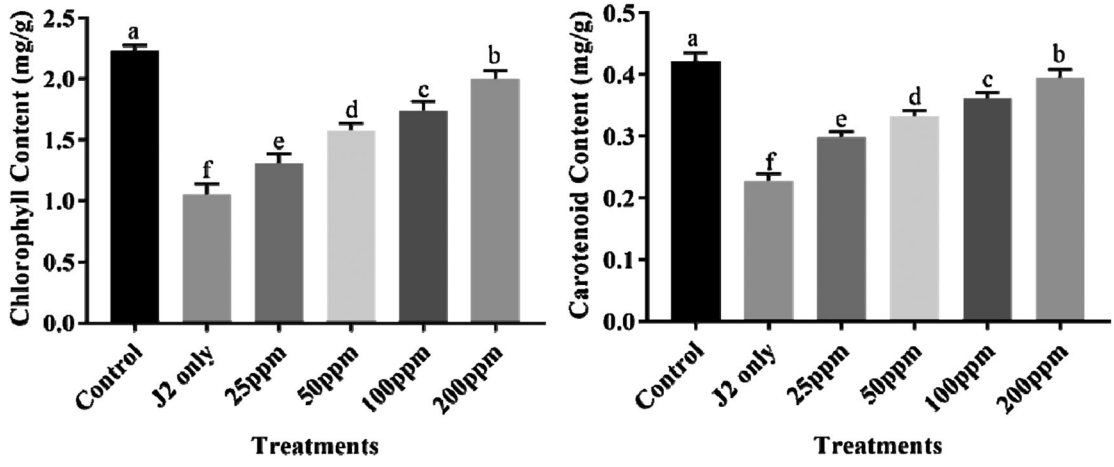

Figure 11. Nematicidal effect of different concentrations of CuONPs on the physiological attributes of J2s inoculated chickpea plants.

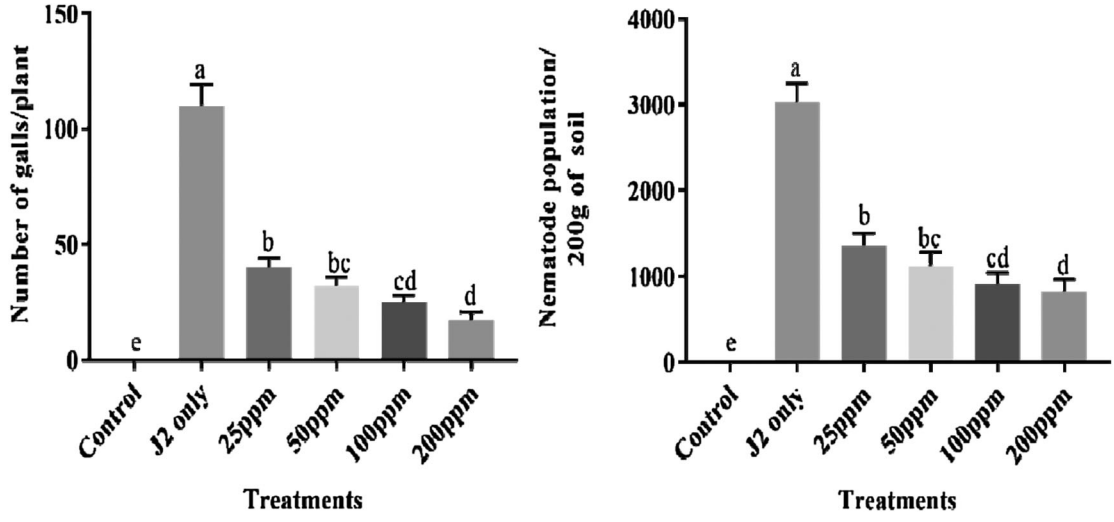

Figure 12. Nematicidal effect of different concentrations of CuONPs on the pathological attributes of J2s inoculated chickpea plants.

negative impact on photosynthesis proportion (*75*). The underlying mechanism of CuONPs action on *M. incognita* is not entirely understood. Many researchers have spent nearly a decade studying complex mechanisms by which metal nanoparticles cause toxicity in bacteria and other microorganisms. The degradation in the cellular structure of nematodes caused by nanoparticles treatment is assumed to be the validation for their massive mortality. Metal oxide nanoparticles may have significant antimicrobial effects by inducing cellular oxidative stress and quickly penetrating the cell wall or membrane, endocytosis, accumulating in the cytoplasm, and eventually causing cell lysis and death (*76*). The toxic effects of nanomaterials are generally associated with the production of lipid-based peroxides and DNA damage related to oxidative stress caused by reactive oxygen species (ROS) (*77*). The mode of action of nanoparticles

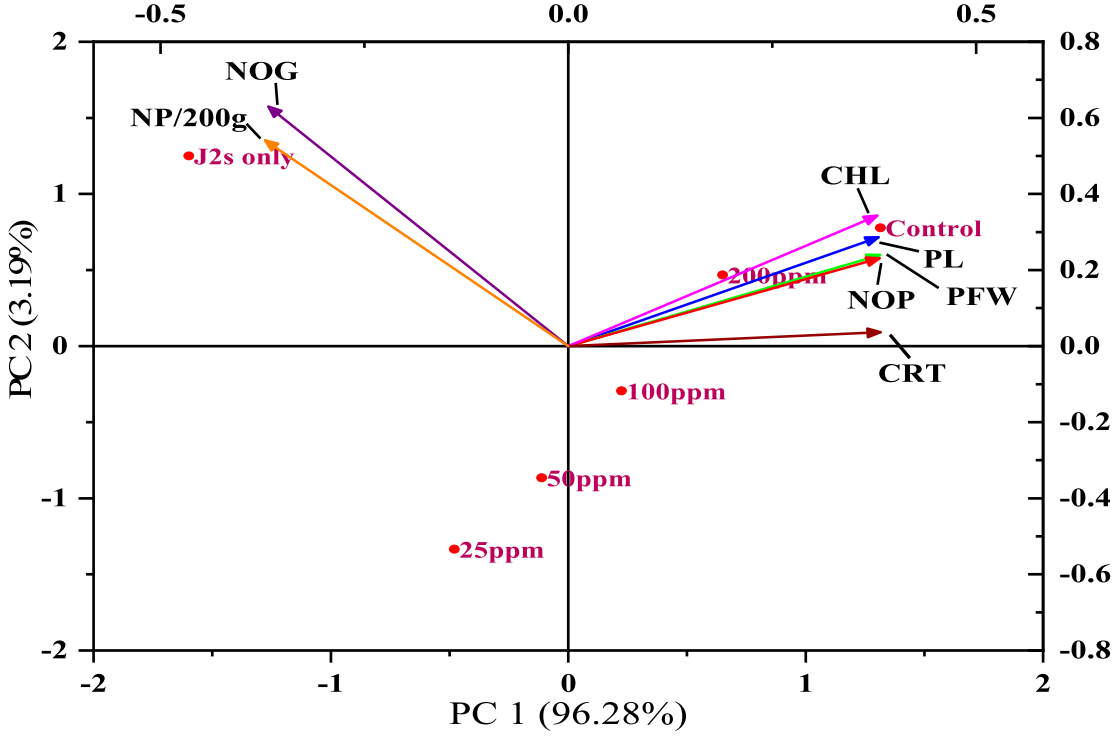

Figure 13. The biplots of principal component analysis, comparing the effects of different concentrations of CuONPs on various studied parameters of J2s inoculated chickpea plants (PFW = Plant fresh weight; PL = Plant length; NOP = Number of pods; CHL = Chlorophyll content; NOG = Number of galls/plant; CRT = Carotenoid content; NP/200g = Nematode population in 200 g soil).

has been likened to cellular mechanisms malfunctioning, allowing cell wall pierces of nematode eggs (*78*). Physical stress-induced cell structure deformation and cell plasma membrane damage linked to nanoparticle cell interactions have also been identified as key sources of toxic effects (*79*). Thus, results revealed that bio-synthesized CuONPs at the appropriate concentration efficiently killed the J2s and reduced the development of root galls in chickpea plants.

4. Conclusions

This study employed a green approach to bio-synthesize CuONPs from the leaf of the *J. curcas* plant. This novel approach is simple, inexpensive and eco-friendly. The J2s of RKN, *M. incognita*, were reactive to green synthesized CuONPs. We noticed that CuONPs significantly killed J2s and inhibited the hatching from egg masses. The root galls of chickpea were also markedly reduced in the pot study when treated with a higher concentration of bio-synthesized CuONPs. However, the higher concentrations of green synthesized CuONPs were more effective under *in vitro* and pot studies. The FTIR results confirmed stabilized CuONPs, and the appearance of some functional groups shifted to a higher value revealed the successful formation of CuONPs. As demonstrated by SEM images, CuONPs were spherical. XRD patterns suggested that the peaks corresponding to 2θ are polycrystalline in nature and have a monoclinic structure of CuONPs. Our findings demonstrate that the bio-synthesis of highly efficient CuONPs *via* simple, effective, and easy pathways would be environmentally friendly and helpful to sustainably manage nematode infection in agriculture crops due to their nematicidal activity. Further study regarding bio-synthesized CuONPs and application at the field level must be carried out to get extensive data about potential nematicidal activity against nematodes and mode of action. So that green synthesized could be used as a possible substitute for chemicals nematicides. However, this study suggests an alternate green tactic to control the RKNs.

Acknowledgement

The authors are thankful to Aligarh Muslim University, Aligarh; for providing facilities to carry out this study.

Disclosure statement

No potential conflict of interest was reported by the author(s).

ORCID

Amir Khan http://orcid.org/0000-0002-6402-8286
Manar Fawzi Bani Mfarrej http://orcid.org/0000-0003-1144-3125
Mohtaram Danish http://orcid.org/0000-0002-2671-2562
Mohammad Shariq http://orcid.org/0000-0002-5439-6595
Mohd. Farhan Khan http://orcid.org/0000-0002-5264-927X
Moh Sajid Ansari http://orcid.org/0000-0002-6279-7444
Mohamed Hashem http://orcid.org/0000-0003-2593-3387
Saad Alamri http://orcid.org/0000-0001-9228-188X
Faheem Ahmad http://orcid.org/0000-0002-7450-0900

References

[1] Khan, M.R.; Ashraf, S.; Rasool, F.; Salati, K.M.; Mohiddin, F.A.; Haque, Z. Field Performance of *Trichoderma* Species Against Wilt Disease Complex of Chickpea Caused by *Fusarium Oxysporum* f. sp. *Ciceri* and *Rhizoctonia Solani*. *Turk. J. Agric. For* **2014**, *38*, 447–454.
[2] Zwart, R.S.; Thudi, M.; Channale, S.; Manchikatla, P.K.; Varshney, R.K.; Thompson, J.P. Resistance to Plant-Parasitic Nematodes in Chickpea: Status and Future Perspectives. *Fron. Plant Sci* **2019,** *10*, 966.
[3] Ali, S.S.; Naimuddin, M., Ali. Nematode infestation in pulse crops Nematode Infestations Part I: Food Crops NatioAcadeScien India. 2010; pp. 288–325.
[4] Kayani, M.Z.; Mukhtar, T.; Hussain, M.A. Evaluation of Nematicidal Effects of *Cannabis Sativa* L. and *Zanthoxylum Alatum* Roxb. Against Root-Knot Nematodes, *Meloidogyne Incognita*. *Crop Prot.* **2012,** *39*, 52–56.
[5] Ahmed, S.; Ahmad, M.; Swami, B.L.; Ikram, S. A Review on Plants Extract Mediated Synthesis of Silver Nanoparticles for Antimicrobial Applications: A Green Expertise. *J. Adv. Res* **2016,** *7*, 17–28.
[6] Haydock, P.P.J.; Woods, S.R.; Grove, I.G.; Hare, M.C. Chemical Control of Nematodes. In: *Plant Nematol CABI Publishing*; Perry, R.N., Moens, M., Eds. Wallingford, **2013**; 259–279.
[7] Van-Viet, P.; Nguyen, H.N.; Cao, T.M.; Van hieu, L. Fusarium Antifungal Activities of Copper Nanoparticles Synthesised by a Chemical Reduction Method. *Nanomat* **2016**, *2016*, Article ID 1957612.
[8] Yuan, J.; Chen, Y.; Li, H.; Lu, J.; Zhao, H.; Liu, M.; Nechitaylo, G.S.; Glushchenko, N.N. New Insights Into the Cellular Responses to Iron Nanoparticles in *Capsicum Annuum*. *Sci. Rep* **2018,** *8*, 3228.
[9] Bindraban, P.S.; Dimkpa, C.; Nagarajan, L.; Roy, A.; Rabbinge, R. Revisiting Fertilisers and Fertilisation Strategies for Improved Nutrient Uptake by Plants. *Biol. Fertil. Soils* **2015,** *51*, 897–911.
[10] Uddin, I. Mechanistic Approach to Study Conjugation of Nanoparticles for Biomedical Applications. *Spectrochim. Acta Part A* **2018,** *202*, 238–243.
[11] Marschner, H.; Marslin, G.; Sheeba, C.J. Mineral Nutrition of Higher Plants. *Fron. Plant. Sci* **2017**, *8*, 832.
[12] Fortunati, E.; Mazzaglia, A.; Balestra, G.M. Sustainable Control Strategies for Plant Protection and Food Packaging Sectors by Natural Substances and Novel Nano Technological Approaches. *J. Sci. Food Agric* **2019,** *99*, 986–1000.
[13] Jeyasubramanian, K.; Thoppey, U.U.G.; Hikku, G.S. Enhancement in Growth Rate and Productivity of

Spinach Grown in Hydroponics with Iron Oxide Nanoparticles. *RSC Adv.* **2016,** *6*, 15451–15459.
[14] Andualem, W.W.; Sabir, F.K.; Mohammed, E.T.; Belay, H.H.; Gonfa, B.A. Synthesis of Copper Oxide Nanoparticles Using Plant Leaf Extract of *Catha Edulis* and its Antibacterial Activity. *J. Nanotechnol* **2020**, *2020*, 1–10. Article ID2932434.
[15] Al-Fa,ouri, A.; Abu-Kharma, M.; Awwad, A. Green Synthesis of Copper Oxide Nanoparticles Using *Bougain Villea* Leaves Aqueous Extract and Antibacterial Activity Evaluation. *Chem. Intern* **2021**, *7* (3), 155–162.
[16] Cuong, H.N.; Pansambal, S.; Ghotekar, S.; Oza, R.; Hai, N.T.T.; Viet, N.M.; Nguye, V.H. New Frontiers in the Plant Extract Mediated Biosynthesis of Copper Oxide (CuO) Nanoparticles and Their Potential Applications: A Review. *Environ. Res* **2022,** *203*, 111858.
[17] Weitz, I.S.; Maoz, M.; Panitz, D.; Eichler, S.; Segal, E. Combination of CuO Nanoparticles and Fluconazole: Preparation, Characterisation, and Antifungal Activity Against *Candida Albicans*. *J. Nanopart. Res* **2015**, *17*, 342.
[18] Jeyasubramanian, K.; Thoppey, U.U.G.; Hikku, G.S.; Selvakumar, N.; Subramania, A.; Krishnamoorthy, K. Enhancement in Growth Rate and Productivity of Spinach Grown in Hydroponics with Iron Oxide Nanoparticles. *RSC Adv.* **2016**, *6*, 15451–15459.
[19] Ingle, A.P.; Duran, N.; Rai, M. Bioactivity, Mechanism of Action, and Cytotoxicity of Copper-Based Nanoparticles: A Review. *Appl. Microbiol. Biotechnol* **2014,** *98*, 1001–1009.
[20] Van-Viet, P.; Nguyen, H.N.; Cao, T.M.; Van hieu, L. Fusarium Antifungal Activities of Copper Nanoparticles Synthesised by a Chemical Reduction Method. *Nanomat* **2016**, *2016*, Article ID 1957612.
[21] Marschner, H.; Marslin, G., Sheeba, C.J., et al. Mineral Nutrition of Higher Plants. *Front Plant. Sci.* **2017**, *8*, 832.
[22] Yruela, I. Copper in Plants: Acquisition, Transport and Interactions. *Funct. Plant Biol.* **2009**, *36*, 409–430.
[23] Ghosh, M.K.; Sahu, S.; Gupta, I.; Ghorai, T.K. Green Synthesis of Copper Nanoparticles from an Extract of *Jatropha Curcas* Leaves: Characterisation, Optical Properties, CT- DNA Binding and Photocatalytic Activity. *RSC Adv.* **2020**, *10*, 22027–22035.
[24] Chauhan, N.; Kumar, P.; Mishra, S.; Verma, S.; Malik, A.; Sharma, S. Insecticidal Activity of *Jatropha Curcas* Extracts Against Housefly, *Musca Domestica*. *Environ Sci Pollut Res Int.* **2015**, *22* (19), 14793–800.
[25] Dumanm, F.; Ocsoy, I.; Kup, F.O. Chamomile Flower Extract-Directed CuO Nanoparticle Formation for its Antioxidant and DNA Cleavage Properties. *Mater. Sci. Eng. C. Mater. Biol. Appl.* **2016,** *60*, 333–338.
[26] De Marco, B.A.; Rechelo, B.S.; Tótoli, E.G.; Kogawa, A.C.; Salgado, H.R.N. Evolution of Green Chemistry and its Multidimensional Impacts: A Review. *Saudi Pharmac J.* **2019**, *27* (1), 1–8.
[27] Sanghi, R.; Singh, V.; Sharma, S.K. Environment and the Role of Green Chemistry. In: Green Chemistry for Environmental Remediation; Sanghi, R., Singh, V., Eds.; Hoboken: John Wiley & Sons, Inc. Salem, MA: Scrivener Publishing LLC, 2011; 1–34.
[28] Gitelson, A.A.; Merzlyak, M.N.; Chivkunova, O.B. Optical Properties and Nondestructive Estimation of Anthocyanin Content in Plant Leaves. *Photochem. Photobiol.* **2001,** *74* (1), 38–45.
[29] Matmin, J.; Affendi, I.; Ibrahim, S.I.; Endud, S. Additive-free Rice Starch-Assisted Synthesis of Spherical Nanostructured Hematite for Degradation of dye Contaminant. *Nanomat* **2018**, *8* (9), 702.
[30] Adhikari, S.; Sarkar, D.; Madras, G. Hierarchical Design of CuS Architectures for Visible Light Photocatalysis of 4-Chlorophenol. *ACS Omega* **2017,** *2* (7), 4009–4021.
[31] Nadeem, H.; Malan, P.; Khan, A.; Asif, M.; Ahmad Siddiqui, M., Angombe, S.T.; Ahmad, F. New Insights on the Utilisation of Ultrasonicated Mustard Seed Cake: Chemical Composition and Antagonistic Potential for Root-Knot Nematode, *Meloidogyne Javanica*. *J. Zhejiang. Univ. Sci. B* **2021**, *22* (7), 563–574.
[32] Abrantes, I.M.O.; Santos, M.S.N.A. A Technique for Preparing Perineal Patterns of Root-Knot Nematodes for Scanning Electron Microscopy. *J.Nematol* **1989**, *21* (1), 138–139.
[33] Aissani, N.; Urgeghe, P.P.; Oplos, C.; Saba, M.; Tocco, G.; Petretto, G.; Eloh, K.; Menkissoglu-Spiroudi, U.; Ntalli, N.; Caboni, P. Nematicidal Activity of the Volatilomeof *Eruca Sativa* on *Meloidogyne Incognita*. *J. Agric. Food Chem* **2015,** *63*, 6120–6125.
[34] Mahesha, H.S.; Ravichandra, N.G.; Rao, M.S.; Narasegowda, N.C. Bio-efficacy of Different Strains of *Bacillus* spp. Against *Meloidogyne Incognita* Under *in Vitro*. *Int. J. Curr. Microbiol. Appl. Sci* **2017**, *6* (11), 2511–2517.
[35] Mackinney, G. Absorption of Light by Chlorophyll Solutions. *J. Biol. Chem* **1941,** *140*, 315–322.
[36] MacLachlan, S.; Zalik, S. Plastid Structure Chlorophyll Concentration and Free Amino Acid Composition of a Chlorophyll Mutant of Barley. *Cana. J. Bot* **1963,** *41*, 1053–1062.
[37] Cobb, N.A. Estimating the Nema Population of Soil, with Special Reference to the Sugar-Beet and Root-Gall Nemas, Heterodera Schachtii Schmidt and Heterodera Radicicola (Greef) MüLler. *Agric Tech Circ Bur Pl Ind US Dep Agric* **1918,** *1*, 48.
[38] Southey, J.F. *Laboratory Methods for Work with Plant and Soil Nematodes*. Ministry of Agriculture, Fisheries and Food: London. Reference Book 1986; 402, p. 202.
[39] Dardiry, M.; Mohamed, A.; Abdelrady, E. Effect of Lead (Pb) on Phytochemical Variability of *Jatropha Curcas* (L.): A Versatile Perennial of Euphorbiaceae Family. *J Biol Stud* **2018,** *1* (3), 133–145.
[40] Solesi, O.A.; Adesina, F.C.; Adebayo-Tayo, B.C.; Abiodun, A.S. Gas Chromatography/Mass Spectrometry (GC-MS) Analysis of *Jatropha Curcas* Latex and its Antimicrobial Activity on Clinical Isolates. *World J Adv Res Rev* **2020,** *8* (1), 012–018.
[41] Cavalcante, N.B.; Santos, A.D.C.; Almeida, J.R.G.S. The Genus *Jatropha* (Euphorbiaceae): A Review on Secondary Chemical Metabolites and Biological Aspects. *Chemico-Biol Interact* **2020,** *318*, 108976.
[42] Rampadarath, S.; Puchooa, D.; Jeewon, R. *Jatropha Curcas* L: Phytochemical, Antimicrobial and Larvicidal Properties. *Asi Paci J Tropi Biomed* **2016**, *6* (10), 858–865.
[43] Khatami, M.; Heli, H.; Jahani, P.M.; Azizi, H.; Nobre, M.A.L. Copper/Copper Oxide Nanoparticles Synthesis Using *Stachys Lavandulifolia* and its Antibacterial Activity. *IET Nanobiotechnol.* **2017**, *11* (6), 709–713.
[44] Zhao, H.; Yang, J.; Wang, L.; Tian, C.; Jiang, B.; Fu, H. Fabrication of a Palladium Nanoparticle/Graphene

Nanosheet Hybrid via Sacrifice of a Copper Template and its Application in Catalytic Oxidation of Formic Acid. *Chem. Commun*. **2011,** *47* (7), 2014–2016.
[45] Chen, D.; Ni, S.; Fang, J.J.; Xiao, T. Preparation of Cu2O Nanoparticles in Cupric Chloride Solutions with a Simple Mechanochemical Approach. *J Alloys Comp* **2010,** *504*, S345–S348.
[46] Guzman, M.; Arcos, M.; Dille, J.; Rousse, C.; Godet, S.; Malet, L. Effect of the Concentration and the Type of Dispersant on the Synthesis of Copper Oxide Nanoparticles and Their Potential Antimicrobial Applications. *ACS Omega* **2021,** *6* (29), 18576–18590.
[47] Mohammadi, S.; Pourseyedi, S.; Amini, A. Green Synthesis of Silver Nanoparticles with a Long Lasting Stability Using Colloidal Solution of Cowpea Seeds (*Vigna* sp. L). *J Environ Chem Eng* **2016,** *4*, 2023–2032.
[48] Bar, H.; Bhui, D.K.; Sahoo, G.P.; Sarkar, P.; De, S.P.; Misra, A. Green Synthesis of Silver Nanoparticles Using Latex of *Jatropha Curcas*. *Coll Surf A Physicochem Eng Asp* **2009,** *339*, 134–139.
[49] Nagar, N.; Devra, V. Green Synthesis and Characterization of Copper Nanoparticles Using *Azadirachta Indica* Leaves. *Mater. Chem. Phys.* **2018,** *213*, 44–51.
[50] Sharma, P.; Pant, S.; Dave, V.; Tak, K.; Sadhu, V.; Reddy, K.R. Green Synthesis and Characterization of Copper Nanoparticles by *Tinospora Cardifolia* to Produce Nature- Friendly Copper Nano-Coated Fabric and Their Antimicrobial Evaluation. *J. Microbiol. Methods* **2019,** *160*, 107–116.
[51] Mali, S.C.; Dhaka, A.; Githala, C.K.; Trivedi, R. Green Synthesis of Copper Nanoparticles Using *Celastrus Paniculatus* Willd. Leaf Extract and Their Photocatalytic and Antifungal Properties. *Biotechnol Rep* **2020**, *27*, e00518.
[52] Shinde, A.B.; Mhamane, D.A.; Nishandar, S.V. Experimental Investigation of Rheological Properties of Water Lubricant by Adding CuO Nanoparticles. *AIP Conf Proce* **2019,** *2200*, 020068.
[53] Zhu, D.; Wang, L.; Yu, W.; Xie, H. Intriguingly High Thermal Conductivity Increment for CuO Nanowires Contained Nanofluids with low Viscosity. *Sci. Rep.* **2018**, *8*, 5282.
[54] Tamuly, C.; Saikia, I.; Hazarika, M.; Das, M.R. Reduction of Aromatic Nitro Compounds Catalysed by Biogenic CuO Nanoparticles. *RSC Adv.* **2014,** *4*, 95.
[55] Kokes, H.; Morcali, M.H.; Acma, E. Dissolution of Copper and Iron from Malachite ore and Precipitation of Copper Sulfate Pentahydrate by Chemical Process. *Eng. Sci. Tech. Int. J* **2014**, *17* (1), 39–44.
[56] Danish, M.; Qamar, M.; Suliman, M.; Muneer, M. Photoelectrochemical and Photocatalytic Properties of Fe@ZnSQDs/TiO2 Nanocomposites for Degradation of Different Chromophoric Organic Pollutants in Aqueous Suspension. *Adv. Com. Hybrid. Mater* **2020,** *3*, 570–582.
[57] Danish, M.; Muneer, M. Excellent Visible-Light-Driven Ni-ZnS/g-C3N4 Photocatalyst for Enhanced Pollutants Degradation Performance: Insight Into the Photocatalytic Mechanism and Adsorption Isotherm. *Appli. Surf. Sci* **2021**, *563*, 150262.
[58] Bouafia, A.; Laouini, S.E.; Ouahrani, M.R. A Review on Green Synthesis of CuO Nanoparticles Using Plant Extract and Evaluation of Antimicrobial Activity. *Asian J Res Chem* **2020,** *13*, 65–70.
[59] Gu, H.; Chen, X.; Chen, F.; Zhou, X.; Parsaee, Z. Ultrasound Assisted Biosynthesis of CuO-NPs Using Brown Alga *Cystoseira Trinodis*: Characterisation, Photocatalytic AOP, DPPH Scavenging and Antibacterial Investigations. *Ultrason. Sonochem.* **2018,** *41*, 109–119.
[60] Mohamed, E.A.; Elsharabasy, S.F.; Abdulsamad, D. Evaluation of *in Vitro* Nematicidal Efficiency of Copper Nanoparticles Against Root-Knot Nematode *M. Incognita*. *S.Asi. J. Parasitol* **2019**, *2* (1), 1–6.
[61] Akhter, G.; Khan, A.; Ali, S.G.; Khan, T.A.; Siddiqi, K.S.; Khan, H.M. Antibacterial and Nematicidal Properties of Biosynthesised Cu Nanoparticles Using Extract of Holoparasiticplant. *SN App. Sci* **2020,** *2*, 1268.
[62] Eloh, K.; Demurtas, M.; Mura, M.G.; Deplana, A.; Onnis, V.; Sasanelli, N.; Maxia, A.; Caboni, P. Potent Nematicidal Activity of Maleimide Derivatives on *Meloidogyne Incognita*. *J. Agric. Food Chem* **2016**, *64*, 4876–4881.
[63] Roh, J.; Sim, S.J.; Yi, J.; Park, K.; Chung, K.H.; Ryu, D.; Choi, J. Ecotoxicity of Silver Nanoparticles on the Soil Nematode *Caenorhabditis Elegans* Using Functional Ecotoxicogenomics. *Environ. Sci. Technol* **2014,** *43*, 3933–3940.
[64] Ahamed, M.; Posgai, R.; Gorey, T.J.; Nielsen, M.; Hussain, S.M.; Rowe, J.J. Silver Nanoparticles Induced Heat Shock Protein 70, Oxidative Stress and Apoptosis in *Drosophila Melanogaster*. *Toxicol. Appl. Pharmacol* **2010,** *242*, 263–269.
[65] Lim, D.; Roh, J.Y.; Eom, H.J.; Choi, J.Y.; Hyun, J.; Choi, J. Oxidative Stress-Related PMK-1 P38 MAPK Activation as a Mechanism for Toxicity of Silver Nanoparticles to Reproduction in the Nematode *Caenorhabditis Elegans*. *Environ. Toxicol. Chem* **2012,** *31*, 585–592.
[66] Ma, H.; Biertsch, P.M.; Glenn, T.C.; Kabengi, N.J.; Williams, P.L. Toxicity of Manufactured Zinc Oxide Nanoparticles in the Nematode *Caenorhabditis Elegans*. *Environ.Toxicol. Chem* **2009,** *28*, 1324–1330.
[67] Chen, P.; Martinez-Finley, E.J.; Bornhorst, J.; Chakraborty, S.; Aschner, M. Metal- Induced Neurodegeneration in *C. Elegans*. *Front Aging Neurosci.* **2013**, *5*, 18.
[68] Baldwin, G.; Bell, A.H. Pararotylenchus n. gen. (Pararotylenchinae n. Subfam., Hoplolaimidae) with six New Species and two new Combinations. *J. Nematol* **1981**, *13* (2), 111–128.
[69] Karlsson, H.L.; Gustafsson, J.; Cronholm, P.; Moller, L. Size-dependent Toxicity of Metal Oxide Particles a Comparison Between Nano- and Micrometer Size. *Toxicol. Lett* **2009,** *188*, 112–118.
[70] Tanyolac, D.; Ekmekci, Y.; Unalan, S. Changes in Photochemical and Antioxidant Enzyme Activities in Maise (*Zea Mays* L.) Leaves Exposed to Excess Copper. *Chemosph* **2007,** *67*, 8998.
[71] El-Magid, A.A.A.; Knany, R.E.; El-Fotoh, H.G.A. Effect of Foliar Application of Some Micronutrients on Wheat Yield and Quality. *Ann. Agric. Sci* **2000,** *1*, 301–313.
[72] Yeon, J.; Park, A.R.; Kim, Y.J.; Seo, H.J.; Yu, N.; Park, H.W.; Kim, J.C. Control of Root-Knot Nematodes by a Mixture of Maleic Acid and Copper Sulfate. *Appli. S. Ecol* **2019,** *141*, 61–68.
[73] Gkanatsiou, C.; Ntalli, N.; Menkissoglu-Spiroudi, U.; Dendrinou-Samara, C. Essential Metal-Based

Nanoparticles (Copper/Iron NPs) as Potent Nematicidal Agents Against *Meloidogyne* spp. *J. Nanotech. Res* **2019,** *1*, 044–058.

[74] Tauseef, A.; Hisamuddin.; Gupta, J.; Rehman, A.; Uddin, I. Differential Response of Cowpea Towards the CuO Nanoparticles Under *Meloidogyne Incognita* Stress. *S. Afric. J. Bot* **2021**, *139*, 175–182.

[75] Nekrasova, G.F.; Ushakova, O.S.; Yermakov, A.; Uymin, M.; Byzov, I.V.; Effects of Coppers (II) Ions and Copper Oxide Nanoparticles on *Elodea Densa* Planch. *Russ. J. Ecol* **2011,** *42*, 458–463.

[76] Raffi, M.; Mehrwan, S.; Bhatti, T.M.; Akhter, J.I.; Hameed, A.; Yawar, W.; ul-Hasan, M.M. Investigations Into the Antibacterial Behaviour of Copper Nanoparticles Against *Escherichia Coli*. *Ann. Microbiol* **2010,** *60*, 75–80.

[77] Meghana, S.; Kabra, P.; Chakraborty, S.; Padmavathy, N. Understanding the Pathway of Antibacterial Activity of Copper Oxide Nanoparticles. *RSC Adv.* **2015,** *5*, 12293–12299.

[78] Sharon, M.; Choudhary, A.K.; Kumar, R. Nanotechnology in Agricultural Diseases and Food Safety. *J. Phytolo* **2010,** *2* (4), 83–92.

[79] Alsammarraie, F.K.; Wang, W.; Zhou, P.; Mustapha, A.; Lin, M. Understanding the Pathway of Antibacterial Activity of Copper Oxide Nanoparticles. *Colloids Surf. B* **2018,** *171*, 398–405.